



## Crosslinkable acrylic-melamine latex produced by miniemulsion polymerization



Carlos A. Córdoba<sup>a</sup>, Sebastián E. Collins<sup>b,c</sup>, Mario C.G. Passeggi Jr.<sup>d,c</sup>, Santiago E. Vaillard<sup>c,e</sup>, Luis M. Gugliotta<sup>a,c</sup>, Roque J. Minari<sup>a,c,\*</sup>

<sup>a</sup> Polymer Reaction Engineering Group, INTEC (Universidad Nacional del Litoral-CONICET), Güemes 3450, Santa Fe 3000, Argentina

<sup>b</sup> Oleochemistry and Catalysis Group, INTEC (Universidad Nacional del Litoral-CONICET), Güemes 3450, Santa Fe 3000, Argentina

<sup>c</sup> Facultad de Ingeniería Química (Universidad Nacional del Litoral), Santiago del Estero 2829, Santa Fe 3000, Argentina

<sup>d</sup> Physics of Surfaces and Interfaces Laboratory, IFIS Litoral (Universidad Nacional del Litoral-CONICET), Güemes 3450, Santa Fe 3000, Argentina

<sup>e</sup> Organic Chemistry Group, INTEC (Universidad Nacional del Litoral-CONICET), Güemes 3450, Santa Fe 3000, Argentina

### ARTICLE INFO

#### Keywords:

Miniemulsion polymerization  
Melamine/acrylic nanocomposites  
Crosslinkable film forming latex

### ABSTRACT

Nowadays, crosslinkable polymers are highly demanded in applications where improved thermal, mechanical, and chemical strengths are required. Among crosslinkable polymers, those with film forming capability (e.g., coatings and adhesives) are of particular interest. This work investigated the miniemulsion polymerization of various acrylic monomer formulations in the presence of an iso-butylated melamine-formaldehyde resin with the aim of obtaining waterborne nanocomposites with controlled crosslinkable capabilities. Variation of the acrylic monomer formulation showed a significant influence on the degree of crosslinking, and consequently, on the final properties of the acrylic/melamine nanocomposite particles, their coalesced films at room temperature and those cured at high temperature. Thereafter, these results offer the opportunity of obtaining waterborne acrylic/melamine nanocomposites with different post-crosslinking capabilities.

### 1. Introduction

The improvement of the thermal, mechanical and physicochemical properties is a crucial challenge for polymer science and technology. In this context, crosslinkable polymers offer a good alternative for satisfying these requirements, where they attempt to both modify and improve known polymers rather than synthesize new polymer materials, representing an attractive option from the scientific, economical and environmental point of view [1]. Among crosslinkable polymers, those with film forming capability are of high technological interest, as coatings or adhesives [2].

In a scenario of increasing concern for sustainability and stricter environmental legislation, the demand of “solvent-free” products is greater than ever. For that reason, coatings industry has switched to water based products, like acrylic latexes. Crosslinkable latexes aim to improve the physical properties of coalesced latex films, over the levels attainable with thermoplastic latexes, which lack hardness, toughness and solvent resistance. From the early articles of Bufkin and Grave [3–8] crosslinkable latexes have been gaining interest. Different types of crosslinking can be potentially used for coating applications, where the reactivity and crosslinking reaction rate can be controlled by

different means (temperature, radiation, and external reactants such as O<sub>2</sub>). Among the employed crosslinkable agents (or crosslinkers), melamine-formaldehyde (MF) resins are widely used in clear-coat industrial applications with hydroxyl, carboxyl and amide functional polymers [9,10].

A reported procedure for preparing crosslinked acrylic/melamine latexes involves the synthesis via emulsion polymerization of an acrylic latex with hydroxyl and/or carboxyl functionalities followed by the inclusion (by physical mixing) of a MF resin [11–16]. This procedure could present various heterogeneity difficulties, depending on the MF resin employed. When a water soluble MF resin is used, most of it remains in the aqueous phase of the latex. On the other hand, the use of a hydrophobic MF resin could promote separated MF droplets stabilized with emulsifier. In both cases, non-uniform latexes can lead to heterogeneous films, which is undesirable, because a MF separated phase can cause non-uniform crosslinking density and mechanical instability. Based on these concepts, Huang and Jones [17] synthesized crosslinkable aqueous-based latexes via emulsion polymerization of acrylic monomers in presence of low molecular weight MF resins (water soluble). While it was found that the presence of MF resins does not significantly interfere with the radical polymerization, it does not

\* Corresponding author at: Polymer Reaction Engineering Group, INTEC (Universidad Nacional del Litoral-CONICET), Güemes 3450, Santa Fe 3000, Argentina.  
E-mail address: [rjminari@santafe-conicet.gov.ar](mailto:rjminari@santafe-conicet.gov.ar) (R.J. Minari).

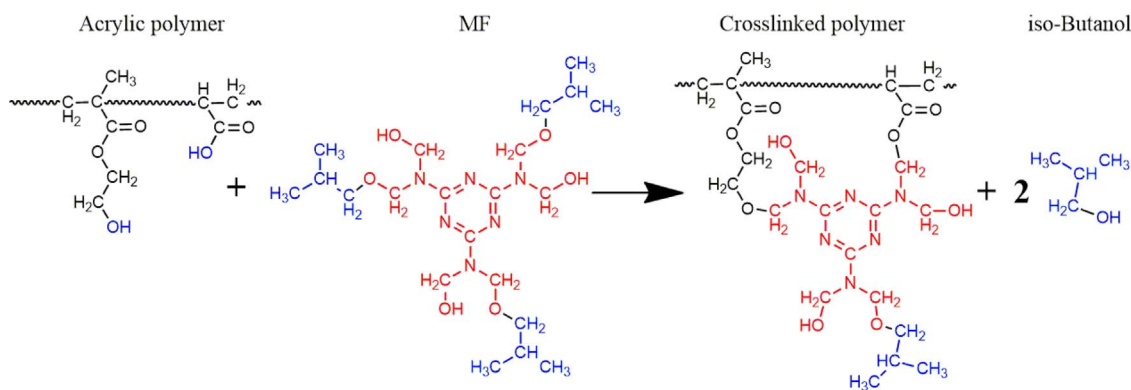


Fig. 1. Scheme of crosslinking reaction between an acrylic polymer containing hydroxyl (from HEMA) and carboxyl (from AA) groups in its backbone and a partially iso-butylated MF.

guarantee their correct incorporation into the polymer particles.

The main reasons for the poorer properties obtained with such latexes compared to the solvent-based counterparts are mainly due to the heterogeneous films formed and to the low molecular weight of MF resin used, which does not guarantee adequate film crosslinking. Solvent borne crosslinkable coatings are formulated containing a hydroxylate acrylic resin of low glass transition temperature ( $T_g$ ), together with a MF resin (soluble in the solvent vehicle). The low  $T_g$  of the acrylic resin allow adequate film formation, improving the mechanical properties by crosslinking at high temperature (curing) between the alkoxy groups of MF resin and the hydroxyls of the acrylic part [18].

Direct miniemulsion polymerization represents an alternative for synthesizing latexes with the incorporation of a hydrophobic component in the polymer particles, avoiding its diffusion through the aqueous phase. Miniemulsion polymerization was successfully employed for obtaining alkyd/acrylic [19], polyurethane/acrylic [20] and polybutadiene/polystyrene nanoparticles [21]. Thus, it would be possible the direct incorporation of a hydrophobic MF resin in a polymer acrylic particle, with the purpose of synthesizing a waterborne nanocomposite with potential application as aqueous crosslinkable latexes, where the use of water as dispersion medium and application vehicle became a more eco-friendly alternative than organic solvent based crosslinkable polymers.

This work investigates the miniemulsion polymerization of a various monomeric acrylic formulations in presence of a commercial iso-butylated MF resin, with the objective of synthesizing crosslinkable acrylic-melamine latexes. It is expected that miniemulsion polymerization ensures an intimate contact between components in order to reach controlled crosslinking in the formed film. The influence of functional monomers onto crosslinking during film formation at room temperature and after post-treatment at high temperature, and onto sensitive properties of the nanocomposite films was exhaustively studied. To the best of our knowledge, the incorporation of melamine resins in acrylic particles by miniemulsion polymerization as a mean of obtaining nano-compatibilized crosslinkable latexes has not previously been studied.

## 2. Experimental

### 2.1. Materials

Potassium persulfate (KPS, Mallinckrodt, 99% purity), and benzoyl peroxide (BPO, AkzoNobel, Perkadox L-W75, containing 25% water), octadecyl acrylate (OA Sigma-Aldrich, 97% purity), Dowfax 2EP (Dow, solution containing 45% of active surfactant), sodium bicarbonate (Cicarelli, 99.7% purity), hydroquinone (Fluka, purity > 99%), hydroxyethylmethacrylate (HEMA, Visiomer Evonik), styrene (St, Petrobras Argentina SA, technical grade), butyl acrylate (BA,

AkzoNobel, technical grade), methyl methacrylate (MMA) and acrylic acid (AA, Sigma-Aldrich), were all used as received from the suppliers. Demineralized water was used throughout the work. The iso-butylated MF resin employed, INDUMEL MF1660 with 60% xylene and traces of iso-butanol (iBOH), was provided by INDUR S.A.C.I.F.I. MF resin was dried under vacuum (5 mmHg) at ambient temperature until constant weight before its use. Tetrahydrofuran (THF, Cicarelli) and methyl ethyl ketone (MEK, Anedra, 99% purity) used as solvents. Chloroform-d<sub>1</sub> (Merck) was used as NMR solvent in the NMR experiments.

### 2.2. Miniemulsification

The following was common to all miniemulsions: a) 20% wt of solids; b) 0.2% w/w (weight based on water) of NaHCO<sub>3</sub> as buffer; and c) 4% w/m (weight based on monomer) of costabilizer (OA). The MF content was 15% w/m in all miniemulsions, with the exception of a melamine-free miniemulsion, taken as reference. The complete acrylic monomeric formulation was based on that reported by Tang et al. [12], which included BA/MMA/St/HEMA/AA (100.0/97.6/26.8/16.3/3.2). At total monomer conversion, it resulted in a polymer with a theoretical  $T_g$  of 16.5 °C. Miniemulsions with different monomer formulations were produced, where the amount of AA and HEMA were varied. AA and HEMA have carboxyl and hydroxyl functionalities, respectively, which can react with methylol and iso-butoxy groups of MF (by curing reaction), forming a crosslinked structure (Fig. 1 schematized the curing reaction). Two different emulsifier (E) concentrations were used for obtaining the miniemulsions, 6 and 2% w/m (i.e., 2.7 and 0.9% w/m of active surfactant) [22].

To produce the miniemulsions the organic and aqueous phases were first strongly mixed by magnetic stirring during 15 min, and then the resulting emulsion was sonified in a Sonics VC 750 apparatus (750 W) at 100% of amplitude, with 20 s on and 5 s off cycles for 35 min. This process was carried out in a 100 mL cooled jacketed vessel, to maintain temperature of the miniemulsion below 35 °C.

### 2.3. Polymerizations

Polymerizations were carried out in a 0.2 L batch glass reactor equipped with a reflux condenser, a stirrer, a sampling device, and a nitrogen inlet. The reaction temperature (70–80 °C) was adjusted by manipulating the reactor jacket temperature with a controlled water bath. The miniemulsion was loaded into the reactor, and the system was kept under stirring and nitrogen bubbling until the desired reaction temperature was reached.

Two different initiators were used: KPS (K experiments) and BPO (B experiments). While KPS was previously dissolved in water and injected into the reactor as a shot to initiate the polymerization, BPO was dissolved in the organic phase before miniemulsification. Notice that KPS generates radicals in the water phase, while BPO produces hydrophobic

radicals in the organic phase. Thus, BPO radicals are restricted to a small phase volume that enhances bimolecular termination, lowering the efficiency of those radicals with respect to the water-soluble KPS radicals [23]. For this reason, B experiments were carried out at higher temperatures (80 °C) than K experiments (70 °C), and at higher initiator concentrations [24] (1.5% wbm) with respect to K experiments (0.8% wbm). The total polymerization time was 3 h in all cases and nitrogen bubbling was maintained during the whole experiment.

## 2.4. Characterization

### 2.4.1. Miniemulsion and latex characterization

<sup>1</sup>H NMR experiments were performed in a Bruker Avance II (300 MHz) spectrometer using CDCl<sub>3</sub> as solvent. Chemical shifts are reported in  $\delta$  units (ppm) using the residual solvent signal as reference (7.27 ppm). The MF resin was characterized by <sup>1</sup>H RMN in phase gel swollen with CDCl<sub>3</sub> [25]. It was found that the MF resin was predominantly monomeric, completely methylolated and partially iso-butylated.

Miniemulsions were characterized by: a) surface tension ( $\gamma$ ) using a Krüss tensiometer model K8; b) colloidal stability, using a Turbiscan (TMA2000), by determining the profile of back scattered light intensity along a vertical tube every 5 min, and during 4 h; and c) average droplets diameter ( $d_d$ ) by dynamic light scattering (DLS) at a detection angle of 90°, in a Brookhaven BI-9000 AT photometer.

Samples withdrawn during polymerization reactions were characterized by: a) total monomer conversion ( $x$ ), by gravimetry; and b) average particles diameter ( $d_p$ ) by DLS. To avoid destabilization of miniemulsions and latexes during DLS measurements, samples were diluted with a water solution saturated with emulsifier, MMA and St. The number of droplets ( $N_d$ ) and particles ( $N_p$ ), and their ratio ( $N_p/N_d$ ) were also calculated from the measurements of  $x$ ,  $d_d$  and  $d_p$ .

The final gel content of latexes, i.e., their insoluble fraction, was determined by directly diluting 0.3 mL of latex in 12 mL of THF during one night and under agitation. Then, the insoluble fraction was separated as a precipitate by centrifugation. The procedure was repeated onto the precipitate extracted with fresh THF. The final precipitate was dried in an oven at 70 °C until constant weight, and the gel fraction was determined taking into account the solid content and  $x$  of the latex.

Particle morphology was determined by TEM, in a JEOL 100 CX (100 kV). Samples of diluted latexes were stained in two steps. First, the diluted latex at 0.01% was treated with 10  $\mu$ L of 2% of Phosphotungstic acid (PTA) solution for 30 min at room temperature to obtain a negative staining of the particle surface. Then, four droplets of the stained diluted latex were placed on copper grids covered with formval (Fluka), and positively stained with vapors of RuO<sub>4</sub> in a closed vessel for 10 min. RuO<sub>4</sub> reacts with amine groups of MF resin, thus staining MF phase.

### 2.4.2. Film characterizations

Minimum film formation temperature (MFFT) of the synthesized latexes was determined employing an optical method [26]. It involved the observation of the clarity of a cast film (60  $\mu$ m thickness) on a large metal table. A temperature gradient was applied to the table and the minimum temperature on it, where the film was judged to be clear, was considered as the MFFT value.

Polymer films used to measure their properties were prepared by casting the latexes onto silicone right-angled moulds; then they were dried at 22 °C and 55% of relative humidity until achieving a constant weight. Dried polymer films were carefully peeled from the silicone substrate, obtaining right-angled films, with a final thickness of about 1 mm. Also, the properties of films treated at 150 °C during 60 min were measured in order to evaluate the effect of curing at high temperature.

The morphology of the films were determined by using a commercial Nanotec Electronic Atomic Force Microscope (AFM) operating in tapping. All the AFM experiments were performed in air at room temperature. Acquisition and image processing were performed using the

WS  $\times$  M free software [27]. Rotated monolithic Budget Sensors All-In-One-Al cantilevers (Budget Sensors, Sofia, Bulgaria) made of silicon with a 30 nm thick aluminum reflex coating and a tip radius < 10 nm were used. The cantilever used have a nominal resonance frequency and spring constant of 350 kHz and 40 N/m, respectively. Cross-sectionals were obtained by (cryo)microtomy (Leica EM UC6).

The insoluble fraction of films samples (FIF) was determined by Soxhlet extraction with THF for 24 h. To evaluate film resistance to water and organic solvent, 20 mm-diameter film samples were immersed in distilled water and MEK, respectively, at room temperature. The relative mass absorbed was calculated after 14 days in the cases where the sample did not present damage.

For tensile tests, film specimens with dumbbell shape of length 9.53 mm and cross Section 3.18 mm  $\times$  1 mm were cut, according to ASTM D882. Test was carried out at an elongation rate of 25 mm/min, according to ASTM D638. Film hardness was correlated with the maximum value of the force measured in compression when the sample was penetrated 1 mm with a 2 mm cylinder plane-probe [28]. Both analyses were carried out in an universal testing machine (INSTRON 3344), at 23 °C and 50% relative humidity. At least five specimens of each sample were tested and average values were reported.

The occurrence of crosslinking reactions was corroborated by in situ transmission infrared spectroscopy. A sample film was prepared by supporting 20  $\mu$ L of latex on a stainless steel mesh (80 wires per inch) and drying it at room temperature for 30 min. The resulting sample was located into a homemade stainless steel transmission cell fitted with CaF<sub>2</sub> windows. Temperature was controlled by two thermocouples, one located into the heating block and other inserted inside the cell space, near the sample. Infrared transmission spectra were acquired with a Nicolet 8700 FTIR spectrometer using an MCT-A detector (resolution 4 cm<sup>-1</sup>, 100 scans). Processing of the spectra was carried out with Omnic 8.0 software. Further evidences of crosslinking was also obtained by NMR onto films obtained from an ad-hoc prepared latex, only containing BA/HEMA in the monomer formulation. The NMR experiments, <sup>1</sup>H, <sup>13</sup>C and heteronuclear <sup>1</sup>H-<sup>13</sup>C correlation (HMBC), were performed onto the film sample swollen with CDCl<sub>3</sub> in a Bruker Avance II 300 MHz spectrometer. Details of the ad-hoc prepared latex and of the NMR characterization are provided in the Supplementary Material.

## 3. Results and discussion

### 3.1. Crosslinkable latex synthesis

The results of the effect of monomer formulation onto polymerization kinetics and polymer microstructure are summarized in Table 1. Second column indicates the particle composition with MF and the monomeric formulation identified with the first letter of each monomer. Also, Fig. 2 presents the evolution of total monomer conversion and average particle size along miniemulsion polymerization. It could be noted that 2 different emulsifier (E) concentrations were used for obtaining the miniemulsions (6 and 2% wbm). It was found that all miniemulsions were stable at room temperature (RT), presenting unaltered backscattering profiles during the 4 h of Turbiscan measurements.

When the highest emulsifier concentration was used, secondary nucleation was predominant, with an important decreasing of  $d_p$  along the polymerization and a final  $N_p/N_d$  higher than 4.5, independently of the initiator type and the monomer recipe. TEM picture for latex K1 (Fig. 3a) confirms the presence of a large fraction of homogenous acrylic particles formed from secondary nucleation together with some core-shell particles, where the dark melamine core was positively stained with ruthenium tetroxide. The use of a reduced emulsifier concentration should favor droplets nucleation [29]. as a consequence of a reduction in the presence of micelles, indicated as an increment in  $\gamma$  (at CMC of DowFax 2EP is equal to 35 mN/m). While droplets were the

**Table 1**  
Synthesis of melamine-based latexes. Effect of monomer formulation on main product characteristics.

Exp.	Particle composition	E [% wbm]	$\gamma$ [mN/m]	$x$ [%]	Latex pH	$d_p$ [nm]	$N_p/N_d$ [-]	Gel [%]
K0	-//M/B/S/H/A	6	35.8	95	4.7	86	4.6	1.3
K1	MF//M/B/S/H/A	6	34.6	79	5.2	69	7.4	16.4
K2	MF//M/B/S	6	–	83	7.9	64	7.0	6.5
K3	MF//M/B/S/A	6	38.0	83	5.3	78	8.7	14.4
K4	MF//M/B/S/H	6	33.7	90	8.2	64	5.8	2.2
K5	MF//M/B/S/H	2	39.7	89	9.0	104	3.6	2.6
B1	MF//M/B/S/H/A	6	34.1	82	5.1	86	4.5	31.6
B2	MF//M/B/S/H	6	35.2	89	7.5	77	4.9	0.8
B3	MF//M/B/S/H	2	38.4	81	7.4	121	1.9	0.5

main site of nucleation when employing BPO and low emulsifier concentration ( $N_p/N_d = 1.9$ , Exp. B3), the contribution of secondary nucleation became increased when using the water soluble KPS ( $N_p/N_d = 3.6$ , Exp. K5). These results are also in agreement with those observed by Ronco et al. [30] where a water soluble initiator promoted secondary nucleation in the miniemulsion polymerization of St (20% solid content). Fig. 3b–c show TEM pictures for latexes K5 and B3. It could be noted that most particles contain the dark phase corresponding to MF while the fraction of homogeneous particles (i.e., without MF) was significantly reduced when comparing with K1 TEM picture (Fig. 3a), thus confirming that miniemulsion droplets nucleation was increased when reducing the emulsifier concentration. While final monomers conversion was not importantly influenced by monomer composition changes, some differences in the polymerization rates were observed when droplets nucleation was increased (i.e., at lower emulsifier concentration). In those cases (B3 and K5) particle size was higher (> 100 nm, also confirmed by TEM) and polymerization rate was slower as it proceeded in the presence of a lower number of polymer particles.

Monomer formulation had an important effect on gel content of latex particles. For example, the presence of monomers containing a reactive functionality with MF, such as H and A, could promote the formation of a crosslinkable structure during polymerization, which

could be identified by the appearance of an insoluble polymer fraction or gel in the polymer particles. Note that when the complete monomer recipe was used (M/B/S/H/A), as in latexes K1 and B1, higher values of gel content were obtained (thus resulting 16.4 and 31.6%, respectively). On the other extreme, the absence of both reactive monomers (H and A) in latex K2 produced a low gel content comparable to that of the melamine-free K0 latex. The simple elimination of H from the monomer formulation, but maintaining A, (latex K3) produced a similar gel content than that observed in K1. A different situation was obtained with a monomer formulation where only A was removed (latexes K4-5 and B2-3). Such latexes presented a low gel content, comparable to that of the melamine-free latex. Note that the enhancement in the distribution of MF through the latex particles by improving droplets nucleation did not practically affect gel content of latexes (compare K4-K5 and B2-B3). It is an indication that the presence of A originated the formation of particles with some crosslinking structures during polymerization. The presence of A in the monomer formulation also gave place to a latex with a pH lower than 7, which could catalyze the melamine crosslinking at room or moderated temperature [31–33].

### 3.2. Film properties and its curing post-treatment at high temperature

Table 2 summarizes the minimum film formation temperature

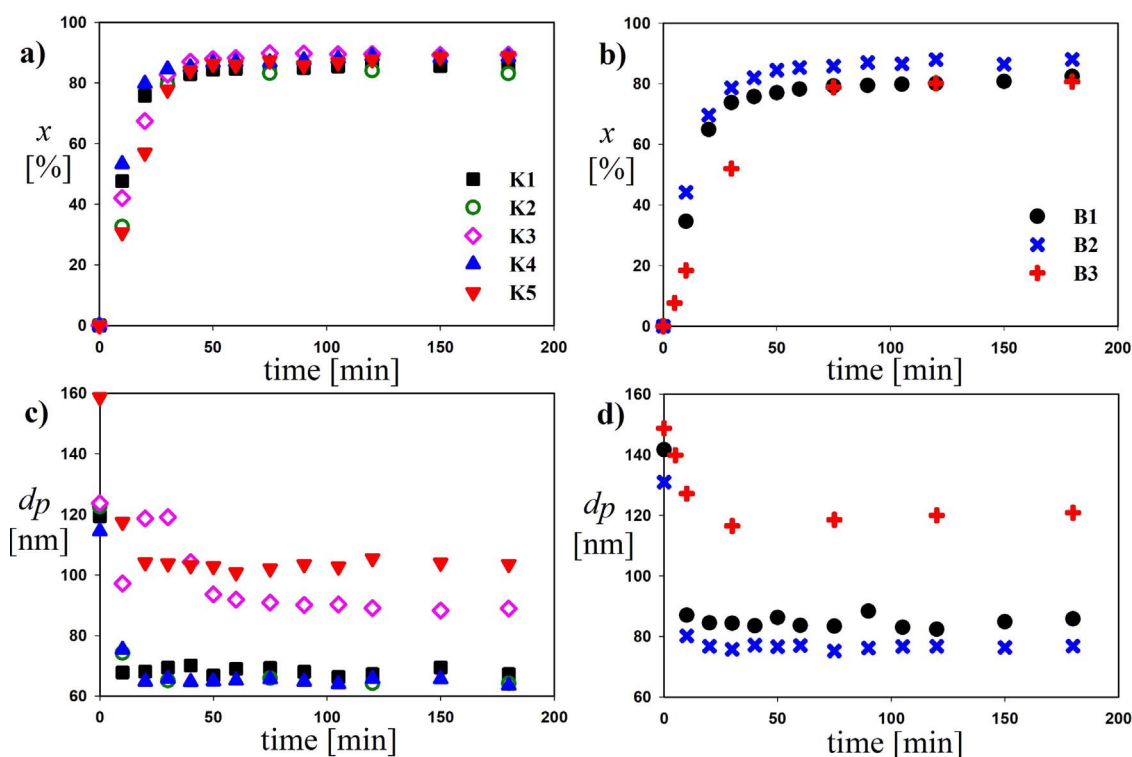


Fig. 2. Evolution of monomer conversion (a, b) and average particle diameter (c, d).

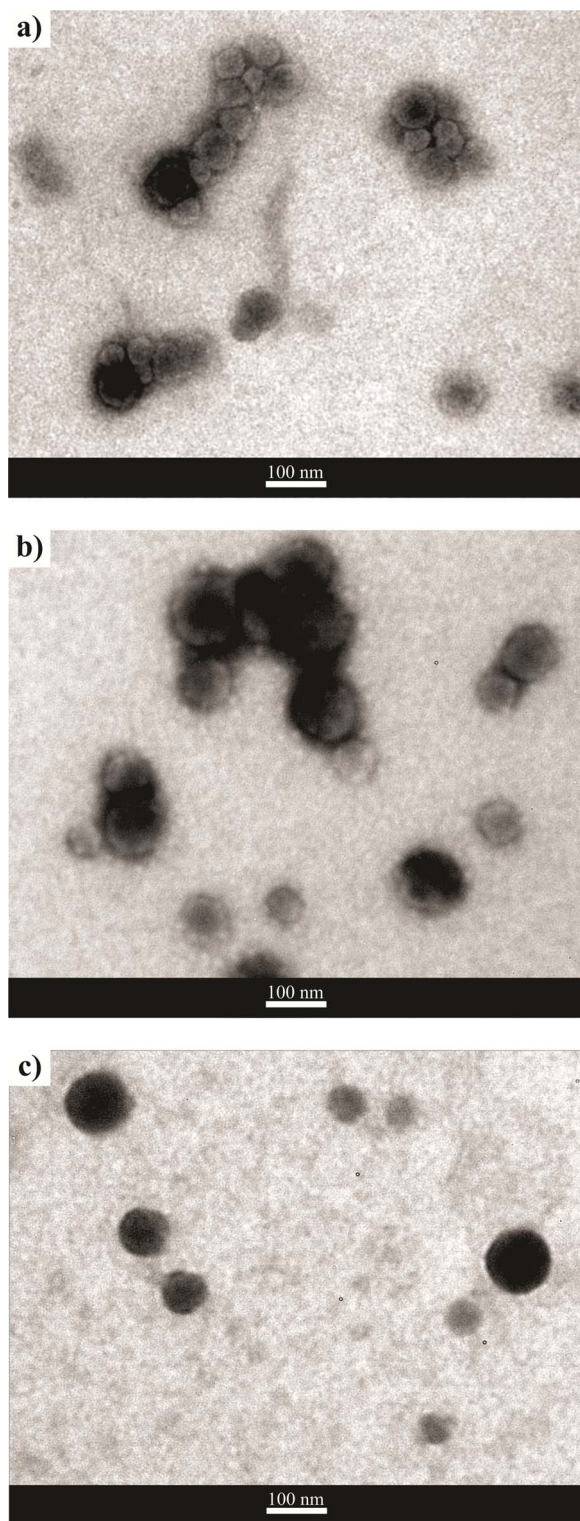


Fig. 3. TEM images for latexes K1 (a), K5 (b) and B3 (c).

(MFFT) for the synthesized latexes and the insoluble fraction (FIF) of films formed at RT and after a curing post-treatment at 150 °C for 60 min. All latexes formed clear films at room temperature, as can be seen in Fig. 4, with a MFFT below 12 °C in all cases. It is noted that the melamine-based films are highly transparent, indicating the absence of big segregated faces in the nanocomposite which could promote light dispersion, i.e., opacity.

The important influence of monomer composition on gel content was previously reported in Section 3.1. Once films were obtained, the

**Table 2**  
MFFT and FIF of melamine-containing films.

Film	MFFT [°C]	FIF [%]	
		Film at RT	Film after curing at 150 °C
K1	9.9	93.9	94.7
K2	11.2	2.0	55.0
K3	10.5	46.0	70.0
K4	7.8	6.7	92.4
K5	8.6	10.2	92.1
B1	8.5	88.2	90.6
B2	4.7	7.0	96.4
B3	2.5	4.2	96.5

FIF values were determined as an indication of the level of crosslinking produced during both film formation at RT, and after curing post-treatment at 150 °C for 60 min. Therefore, a FIF comparable to the latex gel content should be obtained when a low level of crosslinking is produced during film formation or post-treatment. On the other hand, the occurrence of curing reaction should increase the values of FIF with respect to the latex gel content, or with respect to the FIF coalesced film at RT, when such post-treatment process is considered.

Films obtained at RT from latexes K1 and B1, where the complete monomer recipe was used, were almost insoluble, with FIF values of 93.9 and 88.2%, respectively. The absence of H and A in the monomer formulation (i.e., the reactive monomers with MF), in the K2 latex, produced a low FIF value, similar to that of the latex gel content. The simple elimination of H from the monomer formulation in latex K3 allowed maintaining some crosslinking capability during film formation at RT, obtaining a film with FIF close to 50%. However, when A was removed from the monomer formulation (latexes K4-5 and B2-3), they were chemically stable at RT, forming acrylic/melamine films practically without the occurrence of crosslinking reaction (i.e., with FIF values similar to gel contents of latexes). These films should conserve the curing capability for a future post-treatment at high temperature. Consequently, the presence of A in the polymer particle formulation could be an opportunity for obtaining melamine-based latexes with curing capability at RT, in agreement with the previously reported melamine crosslinking catalysis at low temperature due to the presence of acids.

Note that in films where a high crosslinking degree is reached during the drying process at RT (latexes K1 and B1), FIF was not modified by post-treating at 150 °C for 60 min. On the other hand, the occurrence of crosslinking at high temperature produced important changes in FIF for films obtained from latexes without the capability of curing a RT (without A). Also note that the levels of FIF reached when crosslinking occurred were around 90%, regardless of the temperature at which this reaction was carried out (RT or 150 °C). Films K5 and B3 showed similar FIF values (before and after curing) than the homologues K4 and B2, indicating a reduced effect of the MF distribution through the latex particles by improving droplets nucleation.

Final FIF reached in film K3 was 70%, lower than those obtained in other films containing MF, because of the lower availability of reactive monomer (AA). In the case of film K2, where acrylic polymer does not contain functional monomers, the simple self-curing of MF at 150 °C produced a FIF of 55%.

The occurrence of crosslinking was corroborated by FTIR and NMR. Fig. 5 shows, for film K4, the evolution of the FTIR spectra during heating from RT up to 150 °C (at a heating rate of 5 °C/minutes) and after 30 min of post-treatment at 150 °C. Spectra were normalized with the carbonyl group (C=O) of acrylic monomers MMA, BA and HEMA (1652–1772 cm<sup>-1</sup>). This peak remained constant and it was not affected by other absorption peaks during the curing reaction. Fig. 5b shows a detailed view of stretching vibration band of hydroxyl (O–H) groups (3119–3650 cm<sup>-1</sup>). During the first 20 min, the main



Fig. 4. Films K1 (a), B1 (b) and K0 (c).

contribution to the decrease of the intensity in this band was due to the evaporation of residual  $\text{H}_2\text{O}$ . Fig. 5c shows a band around  $2865\text{ cm}^{-1}$  corresponding to the stretching vibrations of aliphatic  $-\text{CH}_3$  and  $-\text{CH}_2$  groups [34]. The decrease in height of the absorption peaks shown in Fig. 5b–c indicates that the hydroxyl (O–H of HEMA) and iso-butoxy ( $(\text{CH}_3)_2\text{CHCH}_2\text{O}-$  of MF) groups were involved in the crosslinking reaction (esquematised in Fig. 1), resulting in the formation of a three-dimensional network structure.

Further evidences of film crosslinking were obtained by HMBC of film samples corresponding to an ad-hoc prepared latex (K5\*, see “Film crosslinking evidence by NMR” section of Supplementary Material). Fig. S1 shows 2D HMBC spectrum for the film formed at RT (in green) and after curing (in red). It could be observed that cross peaks of iso-butoxy group of MF are considerably reduced (and some of them disappear) when the post-treated film is compared with that obtained by coalescence at room temperature. This result suggests that the reduction of the amount of iso-butoxy groups in the post-treated film is consequence of the iso-butanol liberation as by-product in the crosslinking reaction (Fig. 1), which involves the reaction between hydroxyl of HEMA units and the iso-butoxy groups of MF.

Fig. 6 shows the AFM phase images of the cross-section of films K1 and K5 before and after post-treatment at  $150^\circ\text{C}$  for 60 min. For brevity, only phase images are presented as they provide greater image contrast between the soft phase (in dark color) and the hard domains, highly crosslinked regions, (in bright color).

In film K1 at RT (Fig. 6a), it could be mainly observed the presence

of a continuous phase with small hard domains, that coincided in size with those of the particle observed by TEM in Fig. 3a. Also, this hard domains were in agreement with the early observation of the occurrence of crosslinking during film forming. On the other hand, film K5 at RT (Fig. 6c) showed to be an almost homogenous material. When high temperature was applied, both films were hardened, by increasing the appearance of bright domains (Fig. 6b,c). It could be noted the appearance of 3 identifiable phases in film K1 after post-treatment: i) small hard domains which could be a consequence of high local concentration of melamine; ii) soft particles (some of them coalesced) with low content (or lacking) of melamine; and iii) a coalesced continuous phase with an intermediate stiffness and a reduced crosslinking degree with respect to the small hard domains. In cured film K5 (Fig. 6d), the appearance of hard particles (that agreed in size with TEM picture of Fig. 3b) in a coalesced continuous phase with lower stiffness were observed. It is worth pointing out that a greater incidence of curing is observed in K5 film than in K1 film, as it was expected from FIF results (Table 2).

### 3.3. Solvent resistance of films

It is expected that solvent resistance of films, measured as the relative mass absorbed, must be strongly influenced by the degree of crosslinking (Table 3). Pure acrylic film (K0) exhibited a water absorption of around 50% after 14 days of immersion, while it was completely dissolved in MEK (an X indicates that films were disintegrated

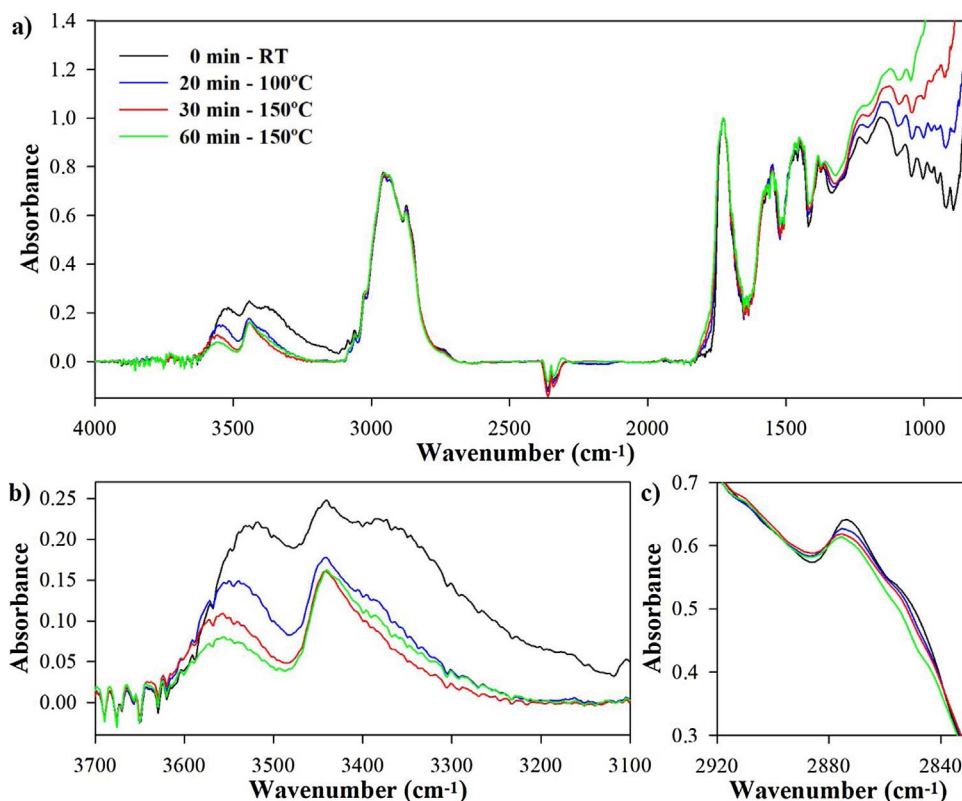


Fig. 5. FTIR spectra of the K4 acrylic/melamine film during the curing process.

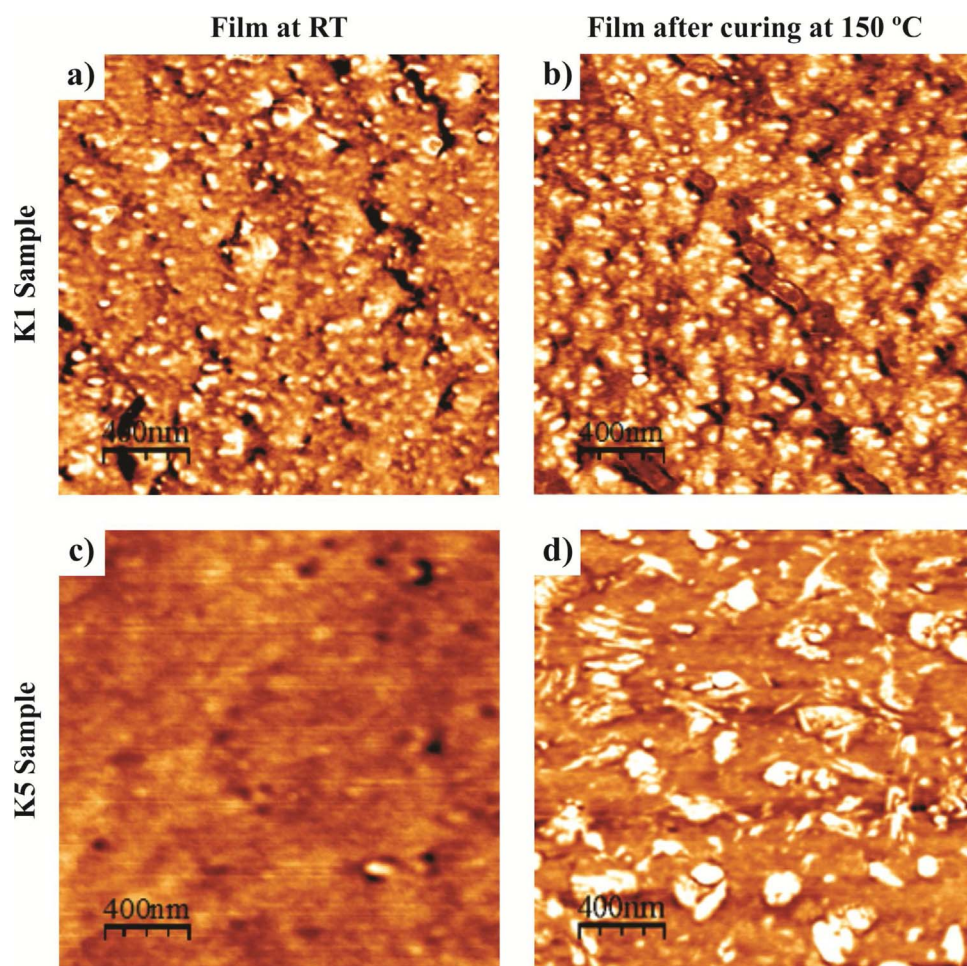


Fig. 6. AFM phase images ( $2.0 \mu\text{m} \times 2.0 \mu\text{m}$ ) of film cross-section for K1 (a,b) and K5 (c,d) samples.

Table 3

Solvent resistance (water and MEK absorption) of melamine-containing films formed at RT and after curing at  $150^\circ\text{C}$ .

Film	Film at RT		Film after curing at $150^\circ\text{C}$	
	Water [%]	MEK [%]	Water [%]	MEK [%]
K0	53.2	X <sup>a)</sup>	–	–
K1	11.6	112.8	22.8	60.0
K3	8.2	182.6	1.0	143.5
K4	81.4	X	39.9	467.6
K5	44.5	X	18.7	352.3
B1	5.4	89.8	11.3	60.0
B2	72.7	1148.1	26.0	240.3
B3	51.4	836.8	22.4	151.0

<sup>a)</sup>X: films disintegrate during assay.

Table 4

Mechanical properties of melamine-containing films.

Film	Film at RT			Film after curing at $150^\circ\text{C}$		
	UTS	Elongation	Hardness	UTS	Elongation	Hardness
	[MPa]	[%]	[N]	[MPa]	[%]	[N]
K0	$9.1 \pm 0.6$	$360 \pm 24.6$	$71.6 \pm 7.2$	–	–	–
K1	$13.4 \pm 2.1$	$121.7 \pm 7.2$	$126.6 \pm 19.1$	$20.5 \pm 0.6$	$165.4 \pm 3.8$	$221.9 \pm 8.4$
K4	$8.1 \pm 0.8$	$297.9 \pm 48.2$	$80.1 \pm 5.8$	$12.9 \pm 4.1$	$283.0 \pm 2.2$	$135.7 \pm 5.6$
K5	$8.6 \pm 0.7$	$332.6 \pm 40.4$	$142.2 \pm 7.9$	$11.8 \pm 1.3$	$294.6 \pm 22.3$	$144.4 \pm 6.5$
B1	$7.7 \pm 0.8$	$143.5 \pm 8.8$	$107.7 \pm 4.8$	$18.5 \pm 1.1$	$157.8 \pm 18.8$	$247.2 \pm 20.2$
B2	$9.6 \pm 0.5$	$400.4 \pm 38.3$	$98.2 \pm 4.8$	$12.3 \pm 0.7$	$225.5 \pm 17.2$	$110.1 \pm 7.9$
B3	$6.2 \pm 0.9$	$345.1 \pm 81.0$	$44.5 \pm 12.1$	$6.7 \pm 0.8$	$81.7 \pm 37.2$	$64.2 \pm 4.6$

during assays). Note that similar performance was observed in melamine-containing films without appreciable crosslinking density at RT, films K4-5 and B2-3 without curing. These films presented a moderate water absorption with a very poor resistance to MEK, where K films were dissolved in MEK (indicated with an X), while B films resisted MEK assays (i.e., 14 days of immersion in MEK), but with a very high level of MEK absorption of around 1000%. It was observed that the increase of crosslinking degree in the acrylic matrix improved the solvent resistance. Films that contained AA in their formulation (K1 and B1), and cured at RT, presented a high resistance to water and MEK immersion with low percentage of swelling. Also, improved solvent resistance was obtained for films K4-5 and B2-3 after curing at  $150^\circ\text{C}$ , that is an additional indication of the increment of crosslinking degree. It is observed that films K5 and B3 exhibited a solvent resistance improvement when compared to their homologues K4 and B2,

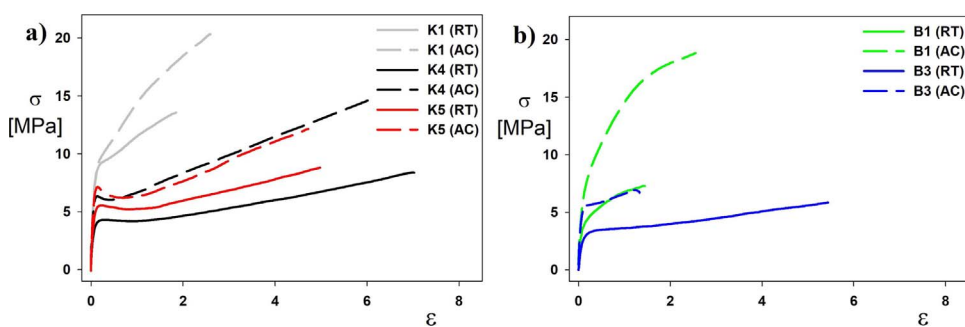


Fig. 7. Stress ( $\sigma$ ) – strain ( $\epsilon$ ) curves for films samples coalesced at RT (in continuous line and indicated as RT), and after curing at 150 °C for 60 min (in dash line and indicated as AC).

respectively. It could be a consequence of the predominant droplets nucleation of latexes K5 and B3, which promoted a more homogenous crosslinking through the films. Note that while FIF of K1 and B1 films did not change after post-treatment, they showed an enhanced MEK resistance. It is an indication that crosslinking density increased during baked.

### 3.4. Mechanical performance of films

Table 4 and Fig. 7 show the results of mechanical performance of MF-containing films formed at RT and after post-treating at 150 °C for 60 min. Film K1 with early crosslinking at RT showed higher ultimate tensile strength (UTS) and hardness, with a reduced elongation capability than film K0. On the other hand, coalesced films K4–K5 and B2–B3, without crosslinking at RT, exhibited comparable mechanical performance (UTS, elongation at break, and hardness) than the free-MF film K0. Crosslinking occurrence through films post-treating at 150 °C for 60 min increased both hardness and UTS and reduced elongation at break. Also, post-treatment of films K1 and B1 improved UTS and hardness, without practically affecting their elongation capability. It was other indication that the maximum crosslinking density was not reached during film coalescence at RT. Notice that post-treated films K4–5 and B2–3 showed higher UTS and lower strengthened than those obtained by latexes coalescence at RT. Despite droplet nucleation was predominant in B3, which enhances MF distribution through the latex particles, mechanical performance was reduced with respect to the homologous B2. It could be due to the lower molar masses of the acrylic polymer that are expected for B3, because of polymerization proceeded under pseudo-bulk conditions with an organic soluble initiator.

## 4. Conclusions

Waterborne acrylic/melamine nanocomposites with post-crosslinking capability were successfully synthesized by miniemulsion polymerization. Despite droplet nucleation (and hence melamine distribution through the latex particles) was varied by adopting two types of initiators (BPO and KPS) and two different emulsifier concentrations, film performance was mainly governed by the acrylic composition. It showed a significant influence on crosslinking and sensitive properties of acrylic/melamine nanocomposite particles, on the coalesced film at room temperature, and on the film cured at high temperature (150 °C). The presence of acrylic acid led to latexes with moderate acid pHs, at which melamine crosslinking at room temperature was catalyzed. Therefore, these acid latexes presented moderated gel contents that could promote the formation of coalesced films at room temperature with high degree of crosslinking, improved solvent resistance and strengthen mechanical properties. These results offer the opportunity of obtaining crosslinkable melamine-based latexes for producing coalesced films cured at room temperature. On the other hand, acrylic formulations only containing hydroxyl functionality (without acrylic acid) produced latexes with low gel content and coalesced films with low crosslinking. Such coalesced films have the possibility of being

cured in a later post-treatment at high temperature, where crosslinking occurs and hence solvent resistance and mechanical strength are enhanced. It was observed that miniemulsion polymerization could be a promising process to obtain waterborne acrylic/melamine nanocomposites with varied post-crosslinking capability for their potential application as coating. Finally, in a future communication the extension of this proposal to high solids that makes this melamine-based latexes of industrial interest will be considered.

## Acknowledgements

The financial support received from CONICET, UNL, and ANPCyT (all of Argentina) is gratefully acknowledged. We also thanks to INDUR S.A.C.I.F.I. for providing the iso-butylated resin employed.

## Appendix A. Supplementary data

Supplementary data associated with this article can be found, in the online version, at <https://doi.org/10.1016/j.porgcoat.2018.01.013>.

## References

- [1] Y. Chai, Y. Zhao, N. Yan, Synthesis and characterization of biobased melamine formaldehyde resins from bark extractives, *Ind. Eng. Chem. Res.* 53 (2014) 11228–11238.
- [2] G. Tillet, B. Boutevinn, B. Ameduri, Chemical reactions of polymer crosslinking and post-crosslinking at room and medium temperature, *Prog. Polym. Sci.* 36 (2011) 191–217.
- [3] B. Bufkin, J. Grawe, Survey of the applications, properties and technology of crosslinking emulsions. 1, *J. Coat. Technol.* 50 (1978) 41–55.
- [4] J. Grawe, B. Bufkin, Survey of the applications, properties and technology of crosslinking emulsions, *J. Coat. Technol.* 2 (50) (1978) 67–83 (Pt. 2).
- [5] B. Bufkin, J. Grawe, Survey of the applications, properties and technology of crosslinking emulsions. 3, *J. Coat. Technol.* 50 (1978) 83–109.
- [6] J. Grawe, B. Bufkin, Survey of the applications, properties and technology of crosslinking emulsions. 4, *J. Coat. Technol.* 50 (1978) 70–100.
- [7] B. Bufkin, J. Grawe, Survey of the applications, properties and technology of crosslinking emulsions. 5, *J. Coat. Technol.* 50 (1978) 65–96.
- [8] J. Grawe, B. Bufkin, Survey of the applications, properties and technology of crosslinking emulsions, *J. Coat. Technol.* 51 (1979) 34–67.
- [9] S.M. Magami, J.T. Guthrie, Amino resin cross-linked can coatings, *Surf. Coat. Int.* 95 (2016) 64–73.
- [10] M.R.L. Paine, N.A. Pianegonda, T.T. Huynh, M. Manefield, S.A. MacLaughlin, S.A. Rice, P.J. Barker, S.J. Blanksby, Evaluation of hindered amine light stabilisers and their N-chlorinated derivatives as antibacterial and antifungal additives for thermoset surface coatings, *Prog. Org. Coat.* 99 (2016) 330–336.
- [11] D.C.K. Chang, Process for improving the appearance of a multilayer finish, U.S. Patent No 4, 731, 290, Mar. 15, 1988.
- [12] L.S. Tang, M. Zhang, S.F. Zhang, J.Z. Yang, High performance waterborne aminoacrylic coatings from the blends of hydrosols and latexes, *Prog. Org. Coat.* 49 (2004) 54–61.
- [13] X. Liu, X. Fan, M. Tang, Y. Nie, Synthesis and characterization of core-shell acrylate based latex and study of its reactive blends, *Int. J. Mol. Sci.* 9 (2008) 342–354.
- [14] M.D. Soucek, E. Pedraza, Control of functional site location for thermosetting latexes, *J. Coat. Technol. Res.* 6 (2009) 27–36.
- [15] R. Han, Y. Zhang, Studies on performance of cured water-borne melamine-acrylic emulsion coatings, *J. Adhes. Sci. Technol.* 25 (2011) 883–892.
- [16] S. Bas, M.D. Soucek, Comparison of film properties for crosslinked core-shell latexes, *React. Funct. Polym.* 73 (2013) 291–302.
- [17] Y. Huang, F.N. Jones, Synthesis of crosslinkable acrylic latexes by emulsion polymerization in the presence of etherified melamine-formaldehyde (MF) resins, *Prog. Org. Coat.* 28 (1996) 133–141.



- [18] W.R. Zhang, T.T. Zhu, R. Smith, C. Lowe, An investigation on the melamine self-condensation in polyester/melamine organic coating, *Prog. Org. Coat.* 69 (2010) 376–383.
- [19] R.J. Minari, M. Goikoetxea, I. Beristain, M. Paulis, M.J. Barandiaran, J.M. Asua, Post-polymerization of waterborne alkyd/acrylics. Effect on polymer architecture and particle morphology, *Polymer (Guildf)* 50 (2009) 5892–5900.
- [20] A. Lopez, E. Degrandi-Contraires, E. Canetta, C. Creton, J.L. Keddie, M. Asua, Waterborne polyurethane – acrylic hybrid nanoparticles by miniemulsion polymerization: applications in pressure-sensitive adhesives, *Langmuir* 27 (2011) 3878–3888.
- [21] L.I. Ronco, R.J. Minari, L.M. Gugliotta, Hybrid Polystyrene/Polybutadiene latexes with low environmental impact, *Macromol. React. Eng.* 10 (2016) 29–38.
- [22] L.I. Ronco, R.J. Minari, M.C.G. Passeggi, G.R. Meira, L.M. Gugliotta, Toughened polystyrene nanoparticles through high-solids miniemulsion polymerization, *Chem. Eng. J.* 263 (2015) 231–238.
- [23] C. Autran, J.C. De La Cal, J.M. Asua, (Mini)emulsion polymerization kinetics using oil-soluble initiators, *Macromolecules* 40 (2007) 6233–6238.
- [24] L.I. Ronco, R.J. Minari, J.R. Vega, G.R. Meira, L.M. Gugliotta, Incorporation of polybutadiene into waterborne polystyrene nanoparticles via miniemulsion polymerization, *Eur. Polym. J.* 49 (2013) 2635–2644.
- [25] C. Braunschier, C. Hametner, Gel-phase <sup>13</sup>C NMR spectroscopy of selected solid phase systems, *QSAR Comb. Sci.* 26 (2007) 908–918.
- [26] J.L. Keddie, Film formation of latex, *Mater. Sci. Eng. R Rep.* 21 (1997) 101–170.
- [27] I. Horcas, R. Fernández, J.M. Gómez-Rodríguez, J. Colchero, J. Gómez-Herrero, A.M. Baro, WSXM: a software for scanning probe microscopy and a tool for nanotechnology, *Rev. Sci. Instrum.* 78 (2007) 13705.
- [28] M.L. Picchio, M.C.G. Passeggi, M.J. Barandiaran, L.M. Gugliotta, R.J. Minari, Waterborne acrylic-casein latexes as eco-friendly binders for coatings, *Prog. Org. Coat.* 88 (2015) 8–16.
- [29] L.L. Hecht, C. Wagner, Ö. Özcan, F. Eisenbart, K. Köhler, K. Landfester, H.P. Schuchmann, Influence of the surfactant concentration on miniemulsion polymerization for the preparation of hybrid nanoparticles, *Macromol. Chem. Phys.* 213 (2012) 2165–2173.
- [30] L.I. Ronco, R.J. Minari, L.M. Gugliotta, Particle nucleation using different initiators in the miniemulsion polymerization of styrene, *Braz. J. Chem. Eng.* 32 (2015) 191–200.
- [31] M.T. Benson, Density functional investigation of melamine-formaldehyde cross-linking agents. 1. Partially substituted melamine, *Ind. Eng. Chem. Res.* 42 (2003) 4147–4155.
- [32] J.K. Mistry, A.M. Natu, M.R. Van De Mark, Synthesis and application of acrylic colloidal unimolecular polymers as a melamine thermoset system, *J. Appl. Polym. Sci.* 131 (2014) 1–12.
- [33] A.M. Natu, M.R. Van De Mark, Synthesis and characterization of an acid catalyst for acrylic-melamine resin systems based on colloidal unimolecular polymer (CUP) particles of MMA-AMPS, *Prog. Org. Coat.* 81 (2015) 35–46.
- [34] T. Yu, Z. Ren, S. Gong, S. Jiang, C. Chao, X. Li, G. Shen, G. Han, Length-controlled synthesis and the photoluminescence of pre-perovskite PbTiO<sub>3</sub> nanofibers, *CrystEngComm* 16 (2014) 3567–3572.